Current Biology

Parallel Actin-Independent Recycling Pathways Polarize Cdc42 in Budding Yeast

Highlights

- Cdc42 can polarize in the absence of its GDI and F-actin

- Cdc42 can exchange between membrane and cytoplasm without the GDI

- Modeling suggests that GDI-independent exchange is sufficient for Cdc42 polarization

- Cells lacking the GDI require a Cdc42-directed GAP to polarize Cdc42

Authors

Benjamin Woods, Helen Lai, Chi-Fang Wu, Trevin R. Zyla, Natasha S. Savage, Daniel J. Lew

Correspondence

nsavage@liverpool.ac.uk (N.S.S.), daniel.lew@duke.edu (D.J.L.)

In Brief

Cdc42 concentrates at a cortical site to specify the cell's front. Woods et al. report that Cdc42 can become concentrated via a novel mechanism involving GDI-independent membrane-cytoplasm exchange. Polarization in the absence of the GDI requires a Cdc42-directed GAP but does not require F-actin.

CellPress

Current Biology

Article

Parallel Actin-Independent Recycling Pathways Polarize Cdc42 in Budding Yeast

Benjamin Woods,[1] Helen Lai,[1] Chi-Fang Wu,[1] Trevin R. Zyla,[1] Natasha S. Savage,[2,*] and Daniel J. Lew[1,*]
[1]Department of Pharmacology and Cancer Biology, Duke University Medical Center, Durham, NC 27710, USA
[2]Institute of Integrative Biology, University of Liverpool, Liverpool L69 7ZB, UK
*Correspondence: nsavage@liverpool.ac.uk (N.S.S.), daniel.lew@duke.edu (D.J.L.)
http://dx.doi.org/10.1016/j.cub.2016.06.047

SUMMARY

The highly conserved Rho-family GTPase Cdc42 is an essential regulator of polarity in many different cell types. During polarity establishment, Cdc42 becomes concentrated at a cortical site, where it interacts with downstream effectors to orient the cytoskeleton along the front-back axis. To concentrate Cdc42, loss of Cdc42 by diffusion must be balanced by recycling to the front. In *Saccharomyces cerevisiae*, the guanine nucleotide dissociation inhibitor (GDI) Rdi1 recycles Cdc42 through the cytoplasm. Loss of Rdi1 slowed but did not eliminate Cdc42 accumulation at the front, suggesting the existence of other recycling pathways. One proposed pathway involves actin-directed trafficking of vesicles carrying Cdc42 to the front. However, we found no role for F-actin in Cdc42 concentration, even in *rdi1Δ* cells. Instead, Cdc42 was still able to exchange between the membrane and cytoplasm in *rdi1Δ* cells, albeit at a reduced rate. Membrane-cytoplasm exchange of GDP-Cdc42 was faster than that of GTP-Cdc42, and computational modeling indicated that such exchange would suffice to promote polarization. We also uncovered a novel role for the Cdc42-directed GTPase-activating protein (GAP) Bem2 in Cdc42 polarization. Bem2 was known to act in series with Rdi1 to promote recycling of Cdc42, but we found that *rdi1Δ bem2Δ* mutants were synthetically lethal, suggesting that they also act in parallel. We suggest that GAP activity cooperates with the GDI to counteract the dissipative effect of a previously unappreciated pathway whereby GTP-Cdc42 escapes from the polarity site through the cytoplasm.

INTRODUCTION

The conserved Rho-family GTPase Cdc42 is a key regulator of polarity establishment [1]. During polarization, Cdc42 becomes activated and concentrated at a cortical site that defines the cell's front [2, 3], orienting the cytoskeleton along the front-back axis. In *Saccharomyces cerevisiae*, polarity establishment requires localized Cdc42 activation by the guanine nucleo-

tide exchange factor (GEF) Cdc24 [4]. But how does Cdc42 itself become concentrated? In *Schizosaccharomyces pombe*, GDP-Cdc42 diffuses much more rapidly than GTP-Cdc42 at the membrane [5], so local activation traps Cdc42, yielding local Cdc42 enrichment. However, membrane GDP-Cdc42 and GTP-Cdc42 appear to diffuse at comparable rates in *S. cerevisiae* [6], and proposed concentration mechanisms involve recycling of Cdc42 via the cell interior. One recycling pathway is mediated by the guanine nucleotide dissociation inhibitor (GDI) Rdi1, and the other involves vesicle delivery on actin cables nucleated by the formin Bni1.

The GDI binds and reversibly extracts Cdc42 and other Rho-family GTPases from the membrane to the cytoplasm, where diffusion is rapid [7]. GDI binds preferentially to GDP-Cdc42, endowing GDP-Cdc42 with a faster mobility than GTP-Cdc42 [8]. Local activation of Cdc42 prevents extraction by the GDI, leading to local Cdc42 enrichment. Because Cdc42 is still concentrated at the front in *rdi1Δ* mutants [9], a second mechanism is proposed to deliver Cdc42 on exocytic vesicles that move along actin cables to the polarity site [10]. A role for F-actin is supported by findings that actin depolymerization reduced (in wild-type cells) [11] or abolished (in *rdi1Δ* mutants) [12, 13] Cdc42 concentration.

To address why cells would need two distinct Cdc42-recycling pathways, we examined polarity establishment in mutants lacking either pathway. Although polarization was slowed without the GDI, it was surprisingly unaffected by the absence of actin cables, even in cells lacking the GDI. Instead, Cdc42 was still able to enter the cytoplasm without the GDI, suggesting that a slow Cdc42 cytoplasmic recycling pathway acts in parallel with the GDI.

RESULTS

Polarity sites arise close to the previous division site because landmark proteins localized during division subsequently promote Cdc42 activation via the Ras-family GTPase Rsr1. To facilitate quantification of polarization dynamics (which can be obscured by proximity to the old division site), we imaged *rsr1* mutants [14].

GFP-Cdc42 is partially functional, supporting polarization only at low temperatures [15, 16]. To image healthy cells, we included untagged Cdc42 as well as GFP-Cdc42. As fluorescently tagged Bem1 (a polarity scaffold protein) is fully functional and Bem1 co-concentrates with Cdc42 [16], we used Bem1 probes to corroborate our conclusions.

CellPress

(legend on next page)
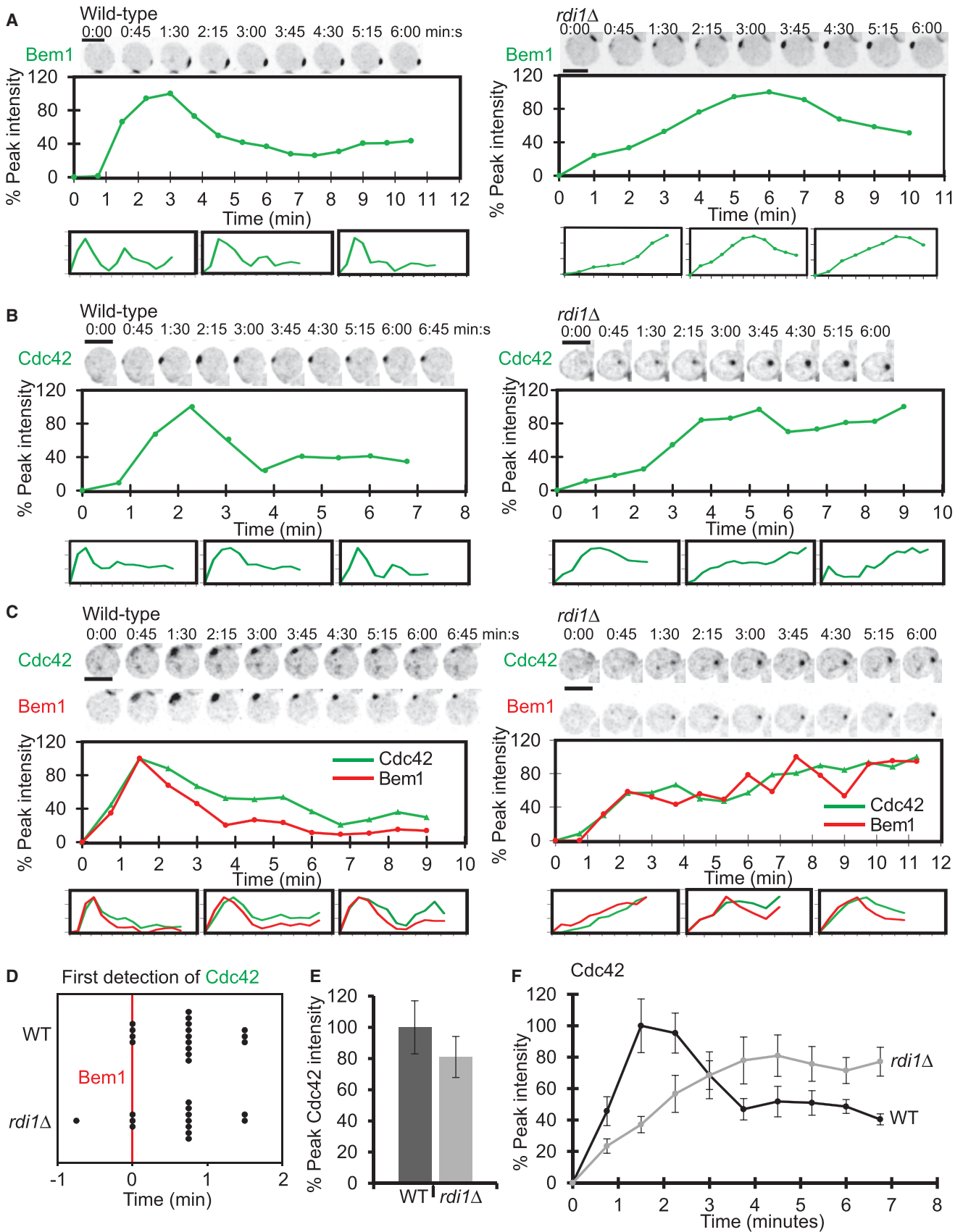
Contribution of the GDI to Polarity Establishment

In wild-type cells, Bem1 and Cdc42 polarized rapidly, reaching peak concentration in ~1 min (Figures 1A and 1B) [17]. Because of a negative feedback loop that reduces GEF activity [18], polarity protein concentrations then decreased and often displayed oscillatory dispersal and re-formation (Figures 1A and 1B; Movie S1). In *rdi1Δ* mutants, Bem1 and Cdc42 polarized more gradually and displayed muted oscillations (Figures 1A and 1B; Movie S1). Two-color imaging suggested that polarization of Cdc42 and Bem1 occurred with similar timing, both in the presence and absence of Rdi1 (Figures 1C and 1D; Movie S2). Imaging of cells with or without Rdi1 on the same slab showed that peak levels of Cdc42 were slightly lower in cells lacking the GDI (Figure 1E), but average Cdc42 accumulation at the time of budding was slightly higher (Figure 1F). Thus, the main effect of deleting *RDI1* is to slow the rate at which polarity factors initially concentrate, suggesting that Cdc42 delivery is rate limiting for polarization.

Contribution of Actin Cables to Polarity Establishment

Actin cables in yeast are nucleated by two formins, Bni1 or Bnr1. Bni1 is localized to the polarity site shortly after Cdc42, whereas Bnr1 is recruited by septins several minutes later [19, 20]. Actin cables can be hard to detect, but they promote concentration of the secretory vesicle-associated Rab, Sec4, at the polarity site. With 54 copies of Sec4 per vesicle [21], GFP-Sec4 provides a sensitive assay for cable polarization. GFP-Sec4 began to accumulate at the polarity site shortly after Bem1 (Figures 2A and 2C; Movie S3) [20], suggesting that Bni1 drives early vesicle delivery. Cells deleted for *BNI1* have cytokinesis defects [22], which might perturb subsequent polarization. To circumvent this, we used temperature-sensitive *bni1-116* [23] mutants. Haploid cells were grown at 24°C, allowing cytokinesis to proceed at permissive temperature, arrested in G1 with pheromone, and released from the arrest at 37°C. Without Bni1, vesicle accumulation at the polarity was delayed (Figures 2B–2D), indicating that Bnr1 did not compensate for the loss of Bni1 at early times. Despite the absence of cables, Bem1 polarization efficiency, peak intensity, and dynamics were unaltered (Figures 2E and 2F), indicating that actin cables do not discernibly contribute to initial polarization.

Actin Depolymerization Affects Polarization Indirectly

Our findings appeared to contradict earlier work using actin depolymerization [11]. We found that polarization efficiency was indeed reduced following exposure to the actin depolymerizing drug latrunculin A (Lat A). But because actin depolymeriza-

tion induces stress responses [24], we wondered whether the impaired polarization might be due to stress. Many stresses delay the cell cycle in G1 prior to start [25–27]. Passage through start involves G1 CDK activity, which triggers nuclear exit of the transcriptional repressor Whi5 [28, 29]. We found that many cells treated with Lat A retained Whi5 in the nucleus for longer periods than DMSO-treated controls (Figure 2G), suggesting that they were delayed in passing start. However, most Lat A-treated cells polarized Bem1 by 10 min after Whi5 nuclear exit (Figures 2H and 2I). Thus, stress-induced cell-cycle delays account for most of the reduced polarization efficiency in these conditions.

Cdc42 Polarization in the Absence of Both the GDI and Actin Cables

Actin cables might still provide a backup Cdc42-delivery pathway that becomes important in the absence of the GDI. In *rdi1Δ* mutants, Sec4 began to concentrate very soon after Bem1 (Figures 3A and 3B; Movie S3). However, in *rdi1Δ bni1-116* mutants, as in *bni1-116* single mutants, vesicle delivery was delayed by several minutes at 37°C (Figure 3C). Bem1 accumulation was slightly reduced in *rdi1Δ bni1-116* mutants, but the timing of Bem1 polarization was unaffected (Figures 3D and 3E). Furthermore, *rdi1Δ bni1Δ* double mutants proliferate successfully (Figure S1). Thus, actin-mediated vesicle delivery does not play a major role in initial polarization, even in the absence of the GDI.

These findings are surprising in light of recent reports that Lat A treatment blocks polarization in *rdi1Δ* mutants [12, 13]. However, we readily detected polarization of GFP-Cdc42 in Lat-A-treated *rdi1Δ* cells (Figures 4A and 4B; Movie S4). Bem1-GFP, Bem1-tdTomato, and Cdc24-GFP probes also polarized in these conditions (Figures 4A and 4B; Movies S4 and S5). Comparable results were obtained with diploids or with haploids synchronized by pheromone arrest/release (Figure 4C; Movie S4). Thus, F-actin is dispensable for polarization of mutants lacking the GDI, regardless of probe, ploidy, or synchrony protocol. Given the stresses stemming from Lat A treatment, we speculate that the discrepancy between our findings and those of others may reflect the degree to which stresses might impair polarity between different strains, treatment protocols, or imaging methods.

How Does Cdc42 Polarize without the GDI?

If not by actin-mediated delivery, then how is Cdc42 concentrated in the absence of the GDI? Previous studies detected residual cytoplasmic Cdc42 in cells lacking the GDI [30, 31], and imaging experiments raised the possibility that Cdc42 may be recycled via the cytoplasm in *rdi1Δ* cells (Figure S2; Movie S6). To ask whether GFP-Cdc42 can exchange between membrane

---

Figure 1. Effect of Rdi1 on Polarity Establishment

Inverted images comparing homozygous diploid *RDI1* and *rdi1Δ* cells synchronized by hydroxyurea arrest-release. Time is in min:s, starting just before polarization. The scale bar represents 5 μm.

(A) Initial accumulation of Bem1-GFP is more rapid in wild-type (DLY9200) than in *rdi1Δ* (DLY17301) cells. (Top) Cropped, maximum projection montages are shown. (Middle) Quantification of Bem1-GFP cluster intensity for same cell is shown. (Bottom) Additional examples are shown.

(B) Initial accumulation of GFP-Cdc42 is more rapid in wild-type (DLY17313) than in *rdi1Δ* (DLY17675) cells. Displays are as above.

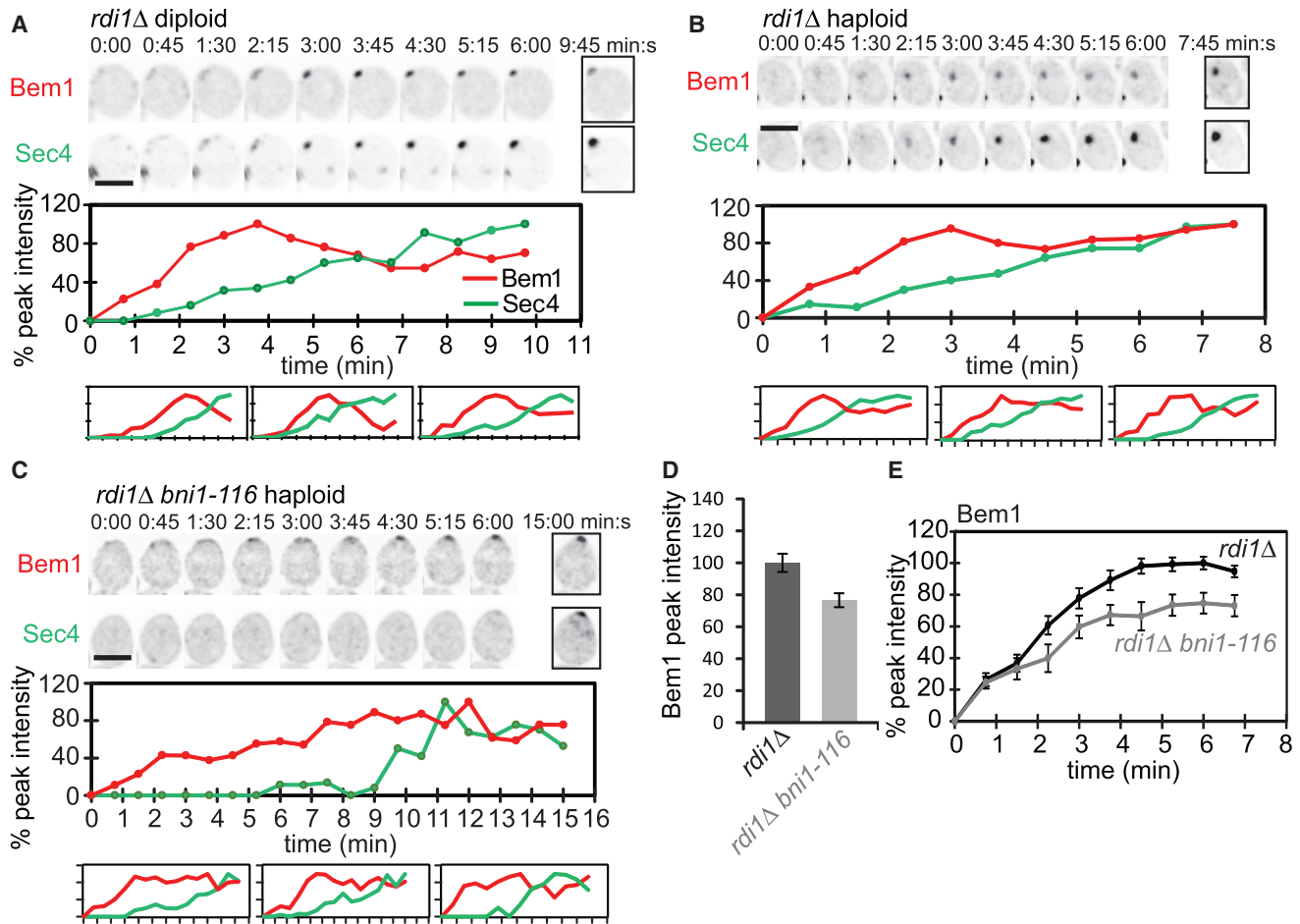(C) Co-accumulation of Bem1-tdTomato and GFP-Cdc42 in wild-type (DLY18067) and *rdi1Δ* (DLY18068) cells.

(D) Time of first detection of Cdc42 clustering, relative to Bem1 clustering (t = 0) in the same cell. Strains are as in (C).

(E) Peak GFP-Cdc42 intensity (mean ± SEM) comparing wild-type (DLY17313; n = 41; normalized to 100) and *rdi1Δ* (DLY17675; n = 19) cells imaged on the same slab.

(F) Accumulation of GFP-Cdc42 (mean ± SEM) in wild-type (DLY17313; n = 14) and *rdi1Δ* (DLY17675; n = 10) cells adjusted for relative peak intensity based on (E).

See also Movies S1 and S2 and Table S1.
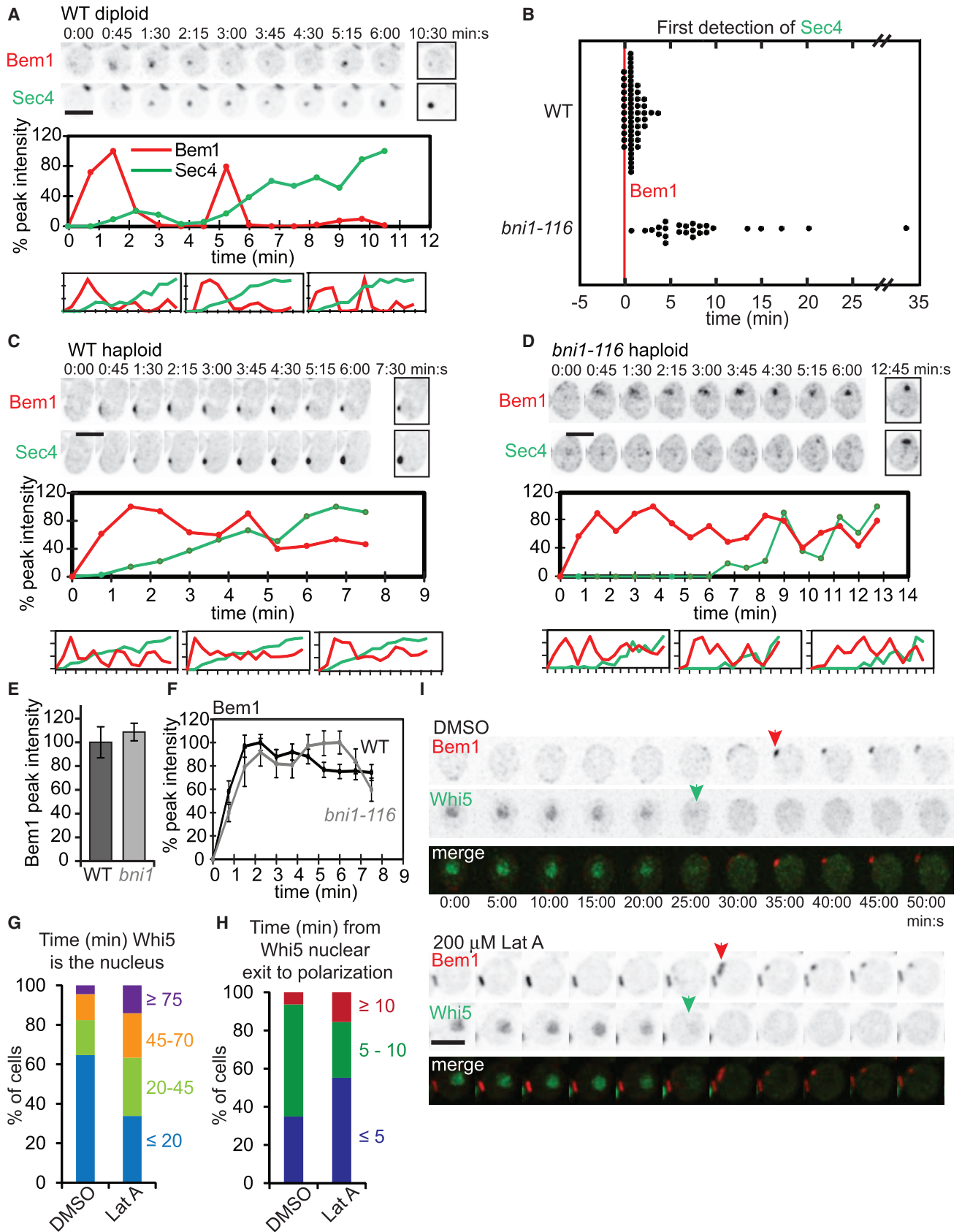
(legend on next page)

**Figure 3. Polarization in the Absence of Rdi1 and Bni1**

(A) Accumulation of Bem1-tdTomato and GFP-Sec4 during polarity establishment in *rdi1*Δ diploids (DLY17317) after hydroxyurea arrest-release. Time is in min:s. The scale bar represents 5 μm.

(B and C) Accumulation of Bem1-tdTomato and GFP-Sec4 in *rdi1*Δ (B; DLY17281) and *rdi1*Δ *bni1-116* (C; DLY20271) haploids after release from pheromone arrest at 37°C.

(D) Peak Bem1-tdTomato intensity (mean ± SEM) comparing *rdi1*Δ (DLY17281 and DLY20054; n = 24 cells; normalized to 100) and *rdi1*Δ *bni1-116* (DLY20271; n = 25 cells) relative to whole-cell fluorescence.

(E) Accumulation of Bem1-tdTomato (mean ± SEM) in *rdi1*Δ (DLY17281; n = 34) and *rdi1*Δ *bni1-116* cells (DLY20271; n = 23) adjusted to relative max intensity.

See also Figure S1, Movie S3, and Table S1.

and cytoplasm without the GDI, we used the "anchor-away" approach [32]. We fused FKBP12 to the ribosomal subunit Rpl13A and the FRB domain from mTOR to GFP-Cdc42 (Figure 5A). The small molecule rapamycin induces tight binding between the FRB and FKBP12 [32], making Cdc42 bind to ribosomes (Figure 5A). If Cdc42 were stuck on membranes, then this would not affect Cdc42 localization. But if Cdc42 exchanges between membrane and cytoplasm, then addition of rapamycin

Figure 2. Effect of Actin Cables on Polarity Establishment

(A) Accumulation of Bem1-tdTomato and GFP-Sec4 during polarity establishment in wild-type diploids (DLY17321) after hydroxyurea arrest-release. Time is in min:s, starting just before polarization. The scale bar represents 5 μm.

(B) First detection of Sec4 relative to Bem1 polarization (t = 0) in wild-type (DLY17282; n = 56) and *bni1-116* (DLY20272; n = 26) cells released from pheromone arrest at 37°C.

(C and D) Polarization of Bem1-tdTomato and GFP-Sec4 in wild-type (C; DLY17282) and *bni1-116* (D; DLY20272) haploids released from pheromone arrest at 37°C.

(E) Peak Bem1-tdTomato intensity (mean ± SEM) comparing wild-type (DLY13040; n = 10) and *bni1-116* (DLY20272; n = 12) cells imaged on the same slab.

(F) Accumulation of Bem1-tdTomato (mean ± SEM) in wild-type (DLY17282; n = 28) and *bni1-116* cells (DLY20272; n = 12) adjusted to relative max intensity.

(G) Proportion of wild-type cells (DLY19237) with nuclear Whi5 for the indicated times in DMSO (n = 68) or 200 μM Lat A (n = 71).

(H) Proportion of wild-type cells (DLY19237) that polarize Bem1 after the indicated time from Whi5 nuclear exit in DMSO (n = 63) or Lat A (n = 58).

(I) Examples of Bem1-tdTomato polarization (red arrow) in DMSO (top) or Lat A (bottom) after Whi5-GFP nuclear exit (green arrow). The scale bar represents 5 μm.

See also Movie S3 and Table S1.

CellPress
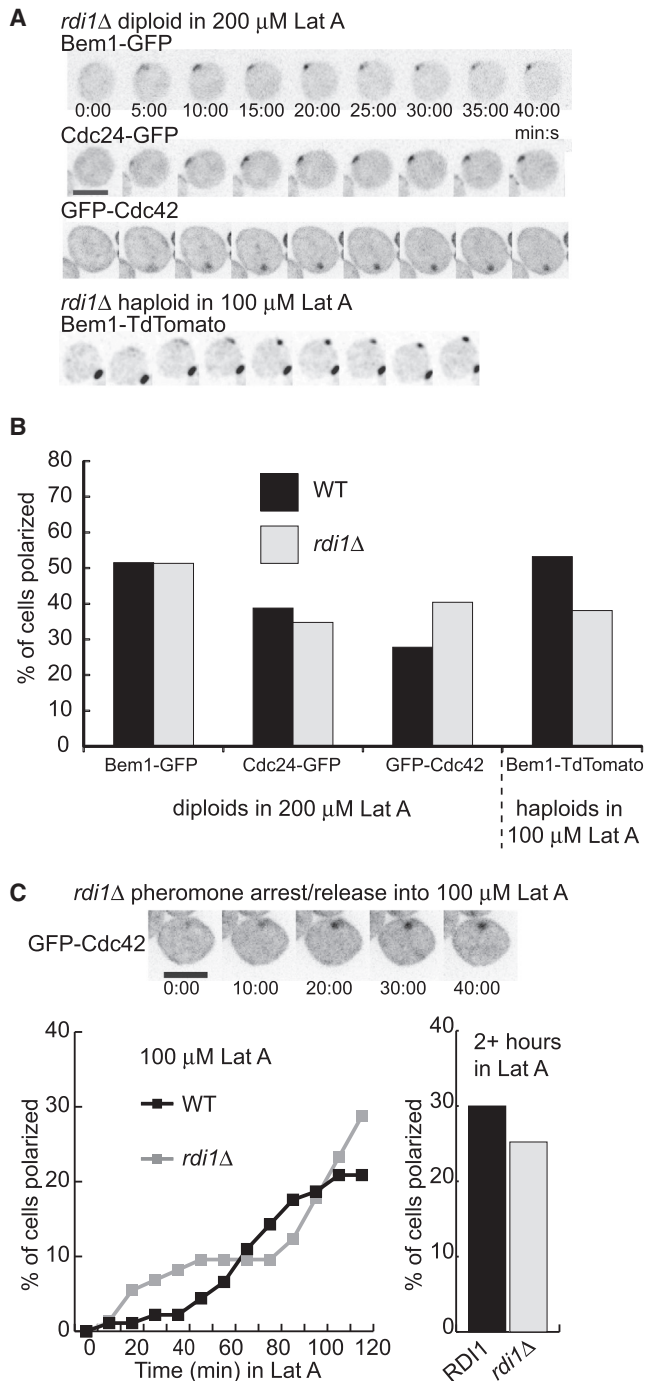
Figure 4. F-actin Is Dispensable for Polarity Establishment in *rdi1Δ* Cells

(A) Inverted, cropped maximum projection montages of *rdi1Δ* cells in Lat A. (From top) Bem1-GFP (DLY17301), Cdc24-GFP (DLY12938), GFP-Cdc42 (DLY17533), and haploid Bem1-tdTomato (DLY19870) are shown.

(B) Quantification of the % of cells that polarized. Wild-type (black) and *rdi1Δ* (gray) diploid cells expressing Bem1-GFP (DLY9200, n = 132; DLY17301, n = 113), Cdc24-GFP (DLY12403, n = 67; DLY12938, n = 69), or GFP-Cdc42 (DLY17532, n = 90; DLY17533, n = 94) were incubated >1 hr on slabs containing 200 μM Lat A. Wild-type and *rdi1Δ* haploid cells expressing Bem1-tdTomato (DLY19237, n = 139; DLY19870, n = 105) were incubated >1 hr on slabs containing 100 μM Lat A.

should trap Cdc42 on cytoplasmic or endoplasmic reticulum (ER)-bound ribosomes. FRB-GFP-Cdc42 was partially functional but became non-functional in the presence of rapamycin (Figure S3). In *rdi1Δ* cells, the protein was localized to membranes, enriched at polarity sites, and detected at low levels in the cytoplasm (Figure 5B). Upon addition of rapamycin, FRB-GFP-Cdc42 relocated to the cytoplasm and internal regions, which seem likely to be rough ER (Figure 5B). In contrast, localization of the plasma membrane protein FRB-GFP-Sso1 was unaffected by rapamycin (Figure S3). Thus, Cdc42 can exchange between membrane and cytoplasm, even in the absence of the GDI. To investigate the potential implications of such exchange, we turned to computational modeling.

GDI-Independent Membrane-Cytoplasm Exchange of GDP-Cdc42 Could Promote Polarization

To address whether slow exchange of Cdc42 between the plasma membrane and the cytoplasm might explain Cdc42 polarization in *rdi1Δ* cells, we began with a model for Cdc42 polarization that incorporates known positive and negative feedback pathways [18, 33–35] (Figure 5C). Because localization of Cdc42 to internal membranes is prominent in *rdi1Δ* mutants (Figure S2A), we added an internal membrane compartment to the model. In the unpolarized steady state, this "*RDI1* model" yields a Cdc42 distribution (Figure 5D) consistent with imaging estimates [11, 15]. In the polarized steady state, this model yields a realistic Cdc42 peak (Figure 5E).

To model the *rdi1Δ* mutant, we assumed that a GDI-independent system would still enable exchange of GDP-Cdc42 at a reduced rate between the cytoplasmic and membrane compartments. Based on western blotting results (Figure 5F), total Cdc42 and Bem1 are equal in *RDI* and *rdi1Δ* models. Rate constants governing the exchange of Cdc42 were constrained by imaging (Figures S2A and S2B) and fluorescence recovery after photobleaching (FRAP) [9] data. We generated a family of models in which cytoplasmic Cdc42 was reduced by 20%, 50%, or 80% (M1, M2, and M3) compared with the *RDI1* model (Figure 5D). These models generated comparable Cdc42 peaks in the polarized steady state, which differed only slightly from the peak in the *RDI1* model (Figure 5E). Thus, a pathway that allows reduced exchange of GDP-Cdc42 between membranes and cytoplasm would suffice to explain the distribution and dynamics of Cdc42 in *rdi1Δ* mutants. To search for potential elements of such a pathway, we performed a genetic screen.

Synthetic Lethal Screen with *rdi1Δ* Mutants Identifies the Rho-GAP *BEM2*

We reasoned that concentrating Cdc42 at the polarity site would be essential for budding, so a pathway facilitating GDI-independent Cdc42 concentration might be dispensable when Rdi1 is available but would become essential in its absence. After random mutagenesis and screening of 1.5 × 10⁵ colonies (see Experimental Procedures), we isolated five mutants that all

(C) (Top) Example *rdi1Δ* haploid cell (DLY17440) released from α-factor arrest into 100 μM Lat A is shown. (Left) % of wild-type (black; DLY17235; n = 91) and *rdi1Δ* cells (gray; DLY17440; n = 73) that polarized GFP-Cdc42 is shown. (Right) Similar quantification from fields that were not used for time-lapse imaging is shown (wild-type, n = 140; *rdi1Δ*, n = 111).
See also Movies S4 and S5 and Table S1.
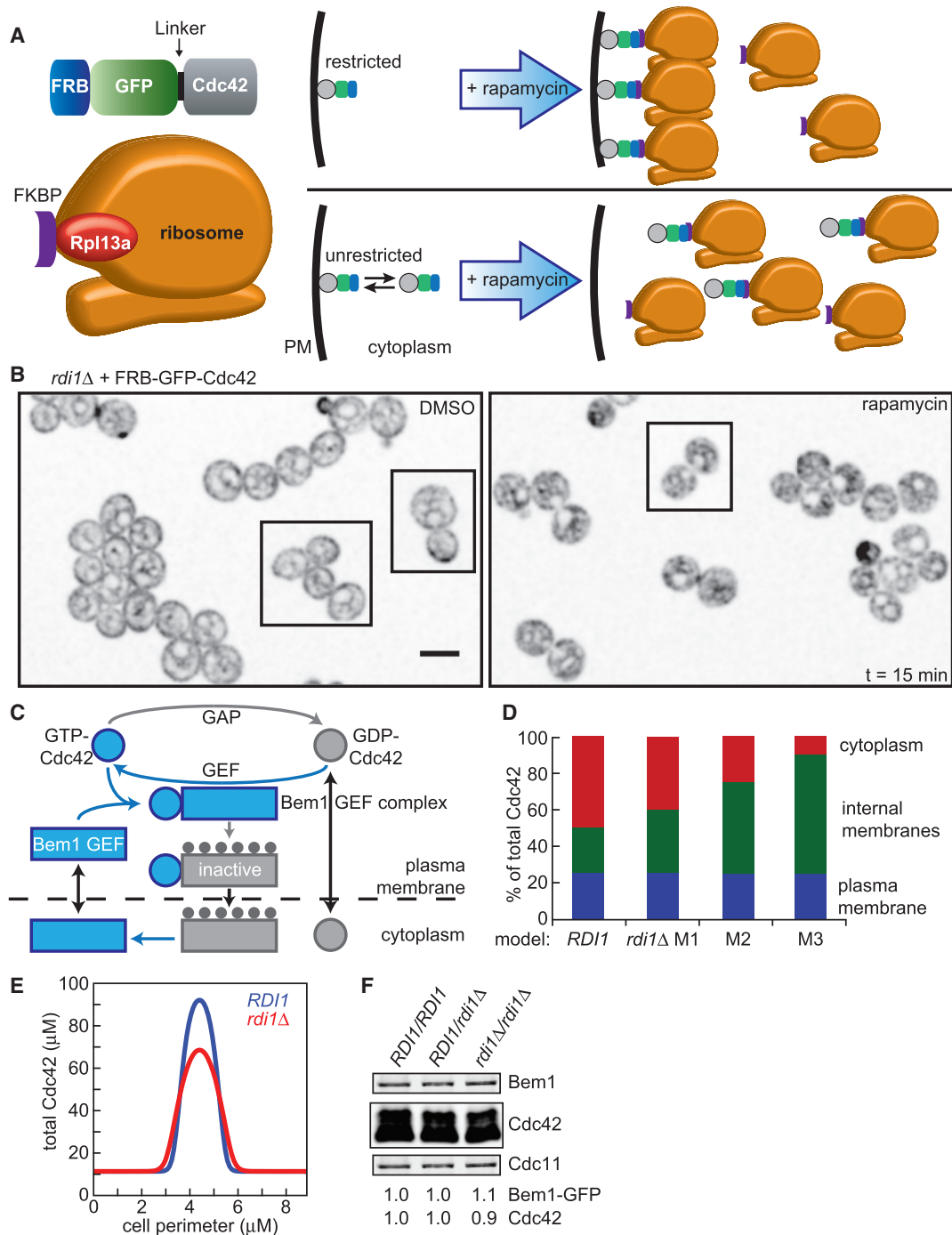
Figure 5. Cdc42 Exchange between Membrane and Cytoplasm without Rdi1

(A) Anchor-away approach. (Left) FRB domains of mTor (blue) and GFP were fused to Cdc42. FKBP12 (purple) was fused to Rpl13a. FRB and FKBP12 bind in the presence of rapamycin. (Right) If FRB-GFP-Cdc42 is always membrane bound, then rapamycin would not alter FRB-GFP-Cdc42 localization. If FRB-GFP-Cdc42 exchanges between membrane and cytoplasm, then rapamycin would trap it in the cytoplasm.

(B) FRB-GFP-Cdc42 localization in control (DMSO) or rapamycin (50 μg/ml)-treated *rdi1Δ* cells (DLY21015). Inverted, single-plane confocal images of cells treated for 15 min at 24°C are shown. The scale bar represents 5 μm.

(C) Reactions in the yeast polarity computational model.

(D) Distribution of Cdc42 among the indicated compartments at the model unpolarized steady state.

(E) Profile of Cdc42 concentration at the model polarized steady state. All *rdi1Δ* models had the same profile.

(F) Blot of Bem1-GFP and Cdc42 in *RDI1/RDI1* (DLY9200), *rdi1Δ/RDI1* (DLY15241), and *rdi1Δ/rdi1Δ* (DLY17301) diploids. Quantification is relative to the Cdc11 loading control.

See also Figures S2 and S3, Movie S6, and Tables S1–S4.
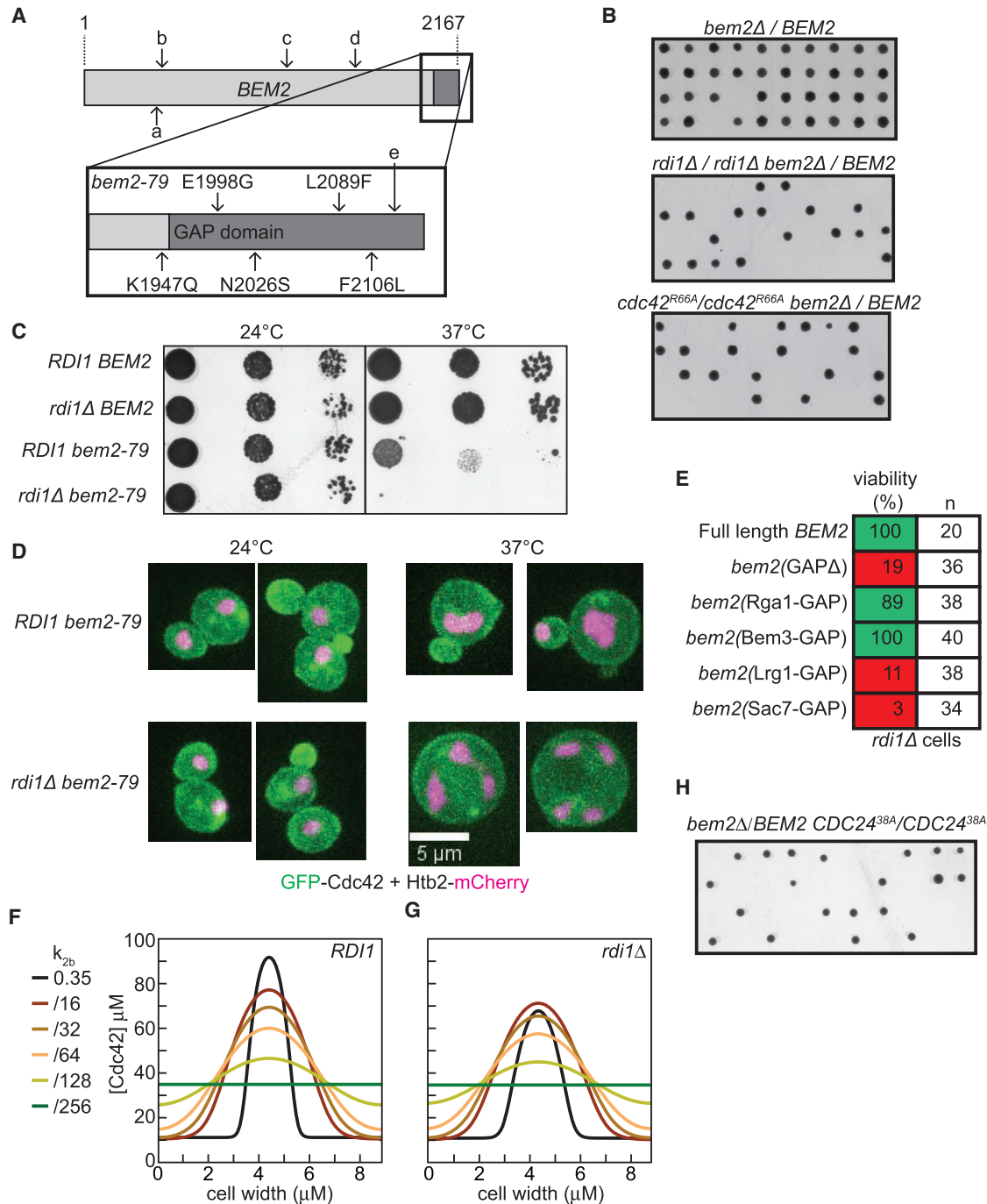
Figure 6. Effect of Cdc42 Exchange and Role of the GAP *BEM2* in *rdi1Δ* Cells

(A) *bem2* alleles a and b harbor non-sense mutations at codons 422 and 445. c and d harbor frameshift mutations at codons 1,177 and 1,570. (Inset) *BEM2* GAP domain is shown. Allele e harbors the missense mutation M2120K. The *bem2-79* temperature-sensitive allele harbors the five indicated mutations.

(B) Deletion of *BEM2* is lethal in *rdi1Δ* and *cdc42^{R66A}* cells. Tetrads from *bem2Δ/BEM2* diploids in either wild-type (DLY8332), *rdi1Δ/rdi1Δ* (DLY15113), or *cdc42^{R66A}/cdc42^{R66A}* (DLY15340) backgrounds. Tetrads are arrayed vertically. All live spores in lower panels were *BEM2*.

(C) *rdi1Δ bem2-79* is lethal at 37°C. Log phase cells (DLY17801, DLY12473, DLY17803, and DLY17802) were spotted and incubated for 2 days at the indicated temperatures on YEPD.

(D) Maximum projection images of *RDI1 bem2-79* (DLY17237) and *rdi1Δ bem2-79* cells (DLY17264) expressing GFP-Cdc42 (green) and the histone Htb2-mCherry (magenta).

(E) Spore viability of *rdi1Δ* cells expressing the indicated Bem2-GAP chimeras, derived from dissection of tetrads from DLY14614, DLY14609, DLY14610, DLY14611, and DLY14746. For strains indicated in red, even viable segregants were very sick.

(legend continued on next page)

mapped to a single gene, *BEM2* (Figure 6A). Bem2 is a 245-kD protein with a Rho- GTPase-activating protein (GAP) domain at its C terminus [36]. Cells lacking *BEM2* are viable, but cells lacking both *RDI1* and *BEM2* are not (Figure 6B).

bem2Δ mutant cells were large, slow growing, and displayed broad patches of Bem1-GFP and GFP-Cdc42 (Movie S7) [37]. Using the temperature-sensitive *bem2-79* (Figure 6A), we found that *rdi1Δ bem2-79* cells arrested as large, round, multinucleate, and mostly unbudded cells, with unpolarized GFP-Cdc42 at restrictive temperature (Figures 6C and 6D). Thus, cells lacking both Rdi1 and Bem2 are unable to concentrate Cdc42.

rdi1Δ bem2Δ Synthetic Lethality Is Due to Defects in Cdc42 GTP Cycling and Trafficking
Rdi1 and Bem2 both regulate Rho1 and Rho4 in addition to Cdc42 [30, 36, 38]. Thus, it was unclear whether *rdi1Δ bem2Δ* synthetic lethality was due to defects in regulating Cdc42 or other Rho GTPases. To address this issue, we generated more-specific mutant strains. Cdc42^{R66A} cannot bind the GDI [39], and *bem2Δ cdc42^{R66A}* cells were inviable (Figure 6B). Next, we replaced the C-terminal GAP domain of Bem2 with the GAP domains of proteins thought to act primarily on Cdc42 (Rga1 or Bem3) or Rho1 (Sac7 or Lrg1) [40–42]. *rdi1Δ* cells expressing Bem2-GAP chimeras specific to Rho1 were very sick or inviable, whereas those with chimeras specific to Cdc42 were much healthier (Figure 6E). These data suggest *rdi1Δ bem2Δ* synthetic lethality arises due to a combined decrease in Cdc42 GTP hydrolysis rate and GDI-mediated Cdc42 mobilization.

Why Would Cells Lacking GDI Need More Cdc42 GAP Activity?
Our results suggest that the GAP Bem2 and GDI Rdi1 operate in parallel to promote Cdc42 polarization. But the GDI preferentially mobilizes GDP-Cdc42, which is the product of GAP action, suggesting that the GAP and GDI should operate in series (a hypothesis supported by FRAP data on GFP-Cdc42 recycling) [12]. How can these observations be reconciled?

To address the effects of reducing GAP activity, we returned to the computational models discussed above and explored the effects of lowering the Cdc42 GTP-hydrolysis rate. In previous work [43], we showed that reducing GAP activity in a model containing positive but no negative feedback would lead to a progressive increase in the peak concentration of Cdc42. However, negative feedback would be expected to buffer such increases [18], and when the same GAP reductions were applied to the full model, peak Cdc42 levels actually decreased slightly (Figure 6F). Reducing GAP activity led to a progressive broadening of the Cdc42 profile, consistent with the very broad polarity peaks observed in *bem2Δ* mutants (Movie S7) [12]. The *RDI1* model tolerated a dramatic 128-fold reduction in GAP activity before polarity collapsed. Consistent with a role for negative feedback in compensating for reduced GAP activity, combination of a non-phosphorylatable GEF (short circuiting the negative feedback loop) [18] and deletion of *BEM2* was synthetically lethal (Figure 6H).

We then investigated the effect of reducing GAP activity in our models of *rdi1Δ* cells (Figure 6G; all three models behaved similarly so only one is shown). Although Cdc42 profiles were broader in *rdi1Δ* models, *RDI1* and *rdi1Δ* models had a similar minimum threshold GAP required for polarization. These simulations confirm, in a quantitatively rigorous manner, the intuitive prediction that, because GAP and GDI act in series, impairment of the GDI should have no further effect once the GAP activity is very low. Why, then, would genetic perturbation of GAP and GDI have synthetic effects? One possibility is that membrane-cytoplasm exchange also occurs for GTP-Cdc42.

GTP-Cdc42 Exchanges Slowly between the Plasma Membrane and the Cytoplasm
To ask whether GTP-Cdc42 could exchange between membrane and cytoplasm, we generated a version of the anchor-away Cdc42 construct (Figure 5A) carrying the GTPase-defective Cdc42^{Q61L} mutant. Expression of Cdc42^{Q61L} at levels comparable to endogenous Cdc42 was lethal, but expression at ~50% the endogenous level is tolerated [44], and we were able to introduce one copy of FRB-GFP-Cdc42^{Q61L} into a diploid strain (Figure 7C). When that diploid was sporulated, all haploids inheriting Cdc42^{Q61L} (and only a single endogenous *CDC42*) were very sick or inviable (Figure 7A). Tetrads dissected on plates containing rapamycin showed full viability (Figure 7A), indicating that induced dimerization of Cdc42^{Q61L} with ribosomes alleviated the toxicity. Cells transferred from rapamycin-containing media to media without rapamycin developed a variety of defects, including large size, large vacuoles, branched and multi-budded cells, and elongated morphology (Figure 7B).

FRB-GFP-Cdc42^{Q61L} was more highly enriched at the plasma membrane than FRB-GFP-Cdc42 (Figure 7D), suggesting that GTP-Cdc42 associates more tightly with the membrane than GDP-Cdc42. Following treatment with rapamycin, FRB-GFP-Cdc42^{Q61L} accumulated internally (Figure 7E), although to a lesser extent than FRB-GFP-Cdc42 (Figure 5B). Thus, although GTP-Cdc42 association with the membrane is tighter than that of GDP-Cdc42, there is still a slow exchange of GTP-Cdc42 between membrane and cytoplasm.

Membrane-Cytoplasm Exchange of GTP-Cdc42 Could Explain *rdi1Δ bem2Δ* Synthetic Lethality
Exchange of GTP-Cdc42 would be expected to dissipate polarity because its high concentration at the polarity site would drive a net flux of GTP-Cdc42 from the polarity site to outlying areas (assuming bound GTP is not hydrolyzed in the cytoplasm). To assess the effects of such a flux, we performed simulations in which membrane-cytoplasm exchange of GTP-Cdc42 was introduced at varying rates (k_{10}). These simulations indicated that such exchange would degrade the polarized peak of Cdc42 (Figure 7F). Significant GTP-Cdc42 exchange could be tolerated without destroying polarity, but once it approached 50% the rate of GDP-Cdc42 exchange, polarity collapsed (Figure 7F). Thus, membrane-cytoplasm exchange of Cdc42 could

(F) Polarized Cdc42 profiles for *RDI1* models with decreasing GAP activity.

(G) Polarized Cdc42 profiles for *rdi1Δ* models with decreasing GAP activity (color as in F).

(H) Deletion of *BEM2* is lethal in cells expressing non-phosphorylatable Cdc24^{38A}. Tetrads from *bem2Δ/BEM2 CDC24^{38A}/CDC24^{38A}* (DLY16303) are shown. See also Movie S7 and Tables S1-S4.
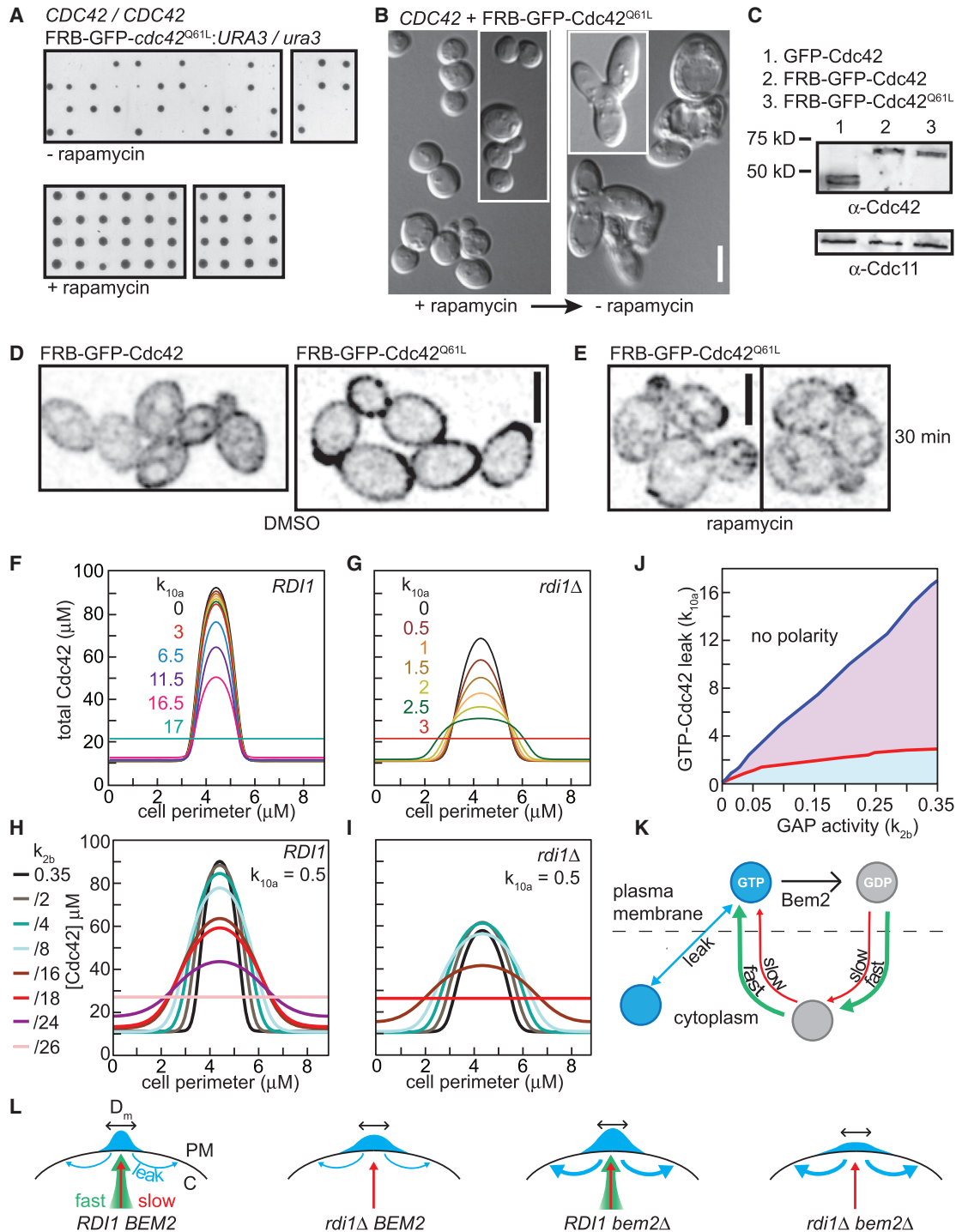
Figure 7. Exchange of GTP-Cdc42 Enhances the Need for GAP Activity in *rdi1Δ* Cells

(A) Tetrads from diploid (DLY21099) heterozygous for FRB-GFP-Cdc42^{Q61L} were dissected on plates with or without rapamycin (20 μg/ml) and incubated for 3 days at 24°C. FRB-GFP-Cdc42^{Q61L} toxicity is rescued by rapamycin.

(B) Differential interference contrast images of haploid FRB-GFP-Cdc42^{Q61L} strain (DLY21130) grown on rapamycin (20 μg/ml; left) or transferred to media lacking rapamycin (right) for 2 days at 24°C. The scale bar represents 5 μm.

(C) Anti-Cdc42 western blot of extracts from cells expressing GFP-Cdc42 (DLY17435), FRB-GFP-Cdc42 (DLY21001), and FRB-GFP-Cdc42^{Q61L} (DLY21099). Cdc11, loading control.

(D) FRB-GFP-Cdc42 ^{Q61L} associates tightly with the plasma membrane. Inverted, single-slice confocal images of diploid cells expressing FRB-GFP-Cdc42 (DLY20963) or FRB-GFP-Cdc42^{Q61L} (DLY21099) are shown. The scale bar represents 5 μm.

(E) FRB-GFP-Cdc42^{Q61L} accumulates internally upon incubation in rapamycin (50 μg/ml at 24°C for 30 min).

(legend continued on next page)

only enable polarization if it occurred significantly faster for GDP-Cdc42 than for GTP-Cdc42.

A similar analysis applied to the *rdi1Δ* models showed that they were much less tolerant of GTP-Cdc42 exchange (Figure 7G). Thus, rapid recycling of GDP-Cdc42 by the GDI is important to effectively combat the dissipative effect of spontaneous GTP-Cdc42 exchange between membrane and cytoplasm.

Might a low-level exchange of GTP-Cdc42 between membrane and cytoplasm explain the need for higher GAP activity in *rdi1Δ* mutants? Models allowing limited GTP-Cdc42 exchange were less tolerant of reduced GAP activity (Figures 7H and 7I). Indeed, increasing GTP-Cdc42 exchange selectively sensitized *rdi1Δ* models to a reduction in GAP activity (Figure 7J). Thus, a plausible explanation for the synthetic lethality of *rdi1Δ bem2Δ* mutants is that loss of the GAP elevates overall GTP-Cdc42 levels, driving a ''leakage'' flux of GTP-Cdc42 through the cytoplasm to outlying membranes and dissipating polarity (Figure 7K). This flux can be counteracted by rapid GDI-mediated recycling of GDP-Cdc42, but not by the slower recycling that occurs in cells lacking the GDI (Figure 7L). Thus, a major role for the GDI may be to provide a rapid recycling of GDP-Cdc42 that compensates for the dissipative effect of spontaneous membrane-cytoplasm exchange of GTP-Cdc42.

DISCUSSION

Our findings suggest two major revisions to current models for Cdc42 polarization in *S. cerevisiae*. First, F-actin is not necessary for Cdc42 polarization and actin cables do not contribute significantly to the first few minutes of polarity establishment, whether or not the GDI is present. These findings are consistent with previous studies that questioned the plausibility of a vesicular pathway for concentrating Cdc42 [35, 45], as well as studies indicating that, in some circumstances, actin can provide a negative feedback on polarity [46].

The proposal that actin cables mediate Cdc42 concentration was supported by experiments showing that eliminating all cables or all F-actin impaired polarization [11–13]. However, these severe perturbations carry the potential to impact polarity through indirect effects. Our findings suggest that Lat A treatment can impair cell-cycle progression, reducing the number of cells that are at the right stage of the cell cycle to polarize. In addition, Lat A treatment induces a Pkc1-mediated stress

response [24] that is known to antagonize polarity, even in cells that have entered the cell cycle [47]. Thus, previous findings may reflect stress responses induced by severe actin perturbation rather than a role of actin in concentrating Cdc42.

By removing the formin Bni1, we generated a situation in which orientation of actin cables and targeted vesicle delivery were delayed by several minutes relative to polarity establishment. However, polarization dynamics were largely unaffected, either in the presence or absence of the GDI, suggesting that actin cables do not contribute to initial polarization.

The second major revision concerns the ability of Cdc42 to exchange between membrane and cytoplasm. Based on physico-chemical considerations, it is often assumed that the polybasic-prenyl C-terminal anchor would effectively lock Cdc42 onto the membrane [48, 49]. However, we find that GFP-Cdc42 does exchange (slowly) between membrane and cytoplasm. This is consistent with previous reports that Cdc42 can transfer spontaneously from one liposome to another in vitro [8]; that the related GTPase, Rac, can exchange between membrane and cytoplasm even after GDI knockdown [50]; and that Rho GTPases (Rho, Rac, and Cdc42) could transfer to the cytoplasm in the absence of the GDI, where they were subject to degradation [51]. Thus, GTPases can dissociate from membranes despite the polybasic-prenyl anchor.

A necessary condition for Cdc42 exchange to promote polarization is that GDP-Cdc42 exchanges more rapidly than GTP-Cdc42. Our computational modeling suggests that, surprisingly, this preference need not be extreme: a significant amount of GTP-Cdc42 exchange could be tolerated without loss of polarity. We found that GTP-locked Cdc42 was more tightly associated with membranes than either wild-type Cdc42 or GFP-polybasic-prenyl anchor. However, it too could transit to the cytoplasm, on a slower timescale. Previous studies similarly detected slow exchange of GTP-Rac in mammalian cells [50]. A simple potential mechanism to slow exchange of GTP-Cdc42 compared to GDP-Cdc42 would be that binding to effectors promotes retention of GTP-Cdc42 at the membrane.

In a genetic screen for factors promoting polarization in parallel with the GDI, we repeatedly isolated the GAP Bem2. Although initially surprising because GAP and GDI activities operate in series to recycle Cdc42, we show that the genetic findings could be explained if we take into account the slow exchange of GTP-Cdc42 between membrane and cytoplasm (Figures 7K and 7L). Such exchange dissipates polarity and has the potential to

(F) Allowing exchange of GTP-Cdc42 between membrane and cytoplasm degrades the polarized peak. Color indicates rate constant for GTP-Cdc42 exchange.

(G) Effect of GTP-Cdc42 exchange on *rdi1Δ* model; color as in (F).

(H and I) Polarized Cdc42 profiles with decreasing GAP activity for *RDI1* (H) or *rdi1Δ* (I) models that allow GTP-Cdc42 exchange.

(J) Parameters governing GAP activity (x axis) and GTP-Cdc42 exchange (y axis) were varied to determine the conditions under which polarity could develop. Lines indicate boundaries between polarizing (lower right) and non-polarizing (upper left) regions of parameter space for *RDI1* (blue line) and *rdi1Δ* (red line) models. For small GTP-Cdc42 exchange rates, the *rdi1Δ* models required more GAP activity than did the *RDI1* model (purple region).

(K) The GDI mediates rapid recycling of GDP-Cdc42 (green), and a GDI-independent pathway mediates slower recycling (red). There is also some ''leakage'' of GTP-Cdc42 (blue). Bem2 works in series with GDI in the recycling pathway but also acts in parallel by limiting the GTP-Cdc42 leak.

(L) Summary model: the Cdc42 peak at the plasma membrane (PM) is maintained by a rapid GDI-mediated influx of GDP-Cdc42 (green arrow) from the cytoplasm (C), and GAP activity limits the dissipative force of a GTP-Cdc42 leak (blue arrows). In *rdi1Δ* cells, reduced influx of GDP-Cdc42 (red arrow) suffices because GTP-Cdc42 leak is limited by GAP activity. In *RDI1 bem2Δ* cells, rapid influx of GDP-Cdc42 can counteract the increased GTP-Cdc42 leak (enlarged blue arrows). In *rdi1Δ bem2Δ* cells, the increased GTP-Cdc42 leak cannot be counteracted by the basal influx of GDP-Cdc42 and polarity fails. D_m is diffusion in the plasma membrane.

See also Figure S3 and Tables S1–S4.

abolish polarity. GAPs and GDIs both act to reduce this "leak" flux of GTP-Cdc42 from the polarity site. GAPs do so by reducing GTP-Cdc42 concentration at the polarity site, reducing the leak; GDIs do so by more rapidly delivering GDP-Cdc42 from the cytoplasm, counteracting the leak.

In conclusion, our work suggests that Cdc42 is recycled through the cytoplasm with or without the GDI. When combined with local activation of Cdc42 [4], such recycling can account for Cdc42 concentration at the polarity site.

EXPERIMENTAL PROCEDURES

Yeast strains, synchrony and imaging methods, and computational modeling are described in Supplemental Information online.

Spot Assay
Cells were grown overnight in liquid media and diluted to 3×10^7 cells ml^{-1}. Ten-fold serial dilutions were spotted onto YEPD plates, starting from 10^4 or 10^5 cells.

Immunoblotting
Total protein was extracted from 10^7 log-phase cells by trichloroacetic acid precipitation. Electrophoresis and western blotting were performed as described [16]. Monoclonal anti-Cdc42 [16] and anti-GFP (Roche Applied Sciences) were used at 1:500 and 1:2,000 dilution. Polyclonal anti-Cdc11 antibodies (Santa Cruz Biotechnologies) and secondary antibodies (IRDye800-conjugated anti-mouse IgG, Rockland Immunochemicals, or Alexa Fluor 680 goat anti-rabbit IgG, Invitrogen) were used at 1:5,000 dilution. Western blots were visualized using the ODYSSEY imaging system (LI-COR Biosciences).

Latrunculin Treatment
Cells were grown in complete synthetic media plus 2% dextrose (CSMD), harvested, resuspended, and mounted onto agarose slabs containing DMSO (control) or latrunculin A (Life Technologies) at 200 μM (asynchronous diploids) or 100 μM (haploids synchronized by pheromone arrest-release). To compare RDI and rdi1 strains, cells were mixed on the same slab. Strains were distinguished either by staining one with 250 μg/ml Concanavalin A Alexa Fluor 594 (Life Technologie s) or by having one strain express HTB2-mCherry.

Light exposure during Lat A treatment was highly toxic, so cells were imaged at either 5- or 10-min intervals. Then, additional (not previously illuminated) cells were also scored for polarization. To confirm the effectiveness of Lat A treatment, additional cells expressing Abp1-mCherry (DLY12120) were spiked into the slab and examined for the absence of actin patches.

Rapamycin Treatment
Cells were grown in CSMD at 24°C and mounted on slabs containing 50 μg/ml rapamycin (or DMSO for controls) for confocal imaging. Alternatively, cells were grown on YEPD agar media with or without 20 μg/ml rapamycin for 2 days, harvested, and mounted on slabs for differential interference contrast imaging.

SUPPLEMENTAL INFORMATION

Supplemental Information includes three figures, four tables, Supplemental Experimental Procedures, and seven movies and can be found with this article online at http://dx.doi.org/10.1016/j.cub.2016.06.047.

AUTHOR CONTRIBUTIONS

B.W., H.L., and C.-F.W. conducted the experiments. B.W., H.L., and T.R.Z. constructed the strains for the experiments. B.W. and D.J.L. designed the experiments and wrote the manuscript with input from H.L. and N.S.S. N.S.S. designed and conducted the computational modeling.

REFERENCES

1. Etienne-Manneville, S. (2004). Cdc42–the centre of polarity. J. Cell Sci. 117, 1291–1300.

2. Ziman, M., Preuss, D., Mulholland, J., O'Brien, J.M., Botstein, D., and Johnson, D.I. (1993). Subcellular localization of Cdc42p, a Saccharomyces cerevisiae GTP-binding protein involved in the control of cell polarity. Mol. Biol. Cell 4, 1307–1316.

3. Richman, T.J., Sawyer, M.M., and Johnson, D.I. (2002). Saccharomyces cerevisiae Cdc42p localizes to cellular membranes and clusters at sites of polarized growth. Eukaryot. Cell 1, 458–468.

4. Woods, B., Kuo, C.C., Wu, C.-F., Zyla, T.R., and Lew, D.J. (2015). Polarity establishment requires localized activation of Cdc42. J. Cell Biol. 211, 19–26.

5. Bendezú, F.O., Vincenzetti, V., Vavylonis, D., Wyss, R., Vogel, H., and Martin, S.G. (2015). Spontaneous Cdc42 polarization independent of GDI-mediated extraction and actin-based trafficking. PLoS Biol. 13, e1002097.

6. Marco, E., Wedlich-Soldner, R., Li, R., Altschuler, S.J., and Wu, L.F. (2007). Endocytosis optimizes the dynamic localization of membrane proteins that regulate cortical polarity. Cell 129, 411–422.

7. Garcia-Mata, R., Boulter, E., and Burridge, K. (2011). The 'invisible hand': regulation of RHO GTPases by RHOGDIs. Nat. Rev. Mol. Cell Biol. 12, 493–504.

8. Johnson, J.L., Erickson, J.W., and Cerione, R.A. (2009). New insights into how the Rho guanine nucleotide dissociation inhibitor regulates the interaction of Cdc42 with membranes. J. Biol. Chem. 284, 23860–23871.

9. Slaughter, B.D., Das, A., Schwartz, J.W., Rubinstein, B., and Li, R. (2009). Dual modes of cdc42 recycling fine-tune polarized morphogenesis. Dev. Cell 17, 823–835.

10. Valdez-Taubas, J., and Pelham, H.R. (2003). Slow diffusion of proteins in the yeast plasma membrane allows polarity to be maintained by endocytic cycling. Curr. Biol. 13, 1636–1640.

11. Wedlich-Soldner, R., Wai, S.C., Schmidt, T., and Li, R. (2004). Robust cell polarity is a dynamic state established by coupling transport and GTPase signaling. J. Cell Biol. 166, 889–900.

12. Freisinger, T., Klünder, B., Johnson, J., Müller, N., Pichler, G., Beck, G., Costanzo, M., Boone, C., Cerione, R.A., Frey, E., and Wedlich-Söldner, R. (2013). Establishment of a robust single axis of cell polarity by coupling multiple positive feedback loops. Nat. Commun. 4, 1807.

13. Smith, S.E., Rubinstein, B., Mendes Pinto, I., Slaughter, B.D., Unruh, J.R., and Li, R. (2013). Independence of symmetry breaking on Bem1-mediated autocatalytic activation of Cdc42. J. Cell Biol. 202, 1091–1106.

14. Wu, C.-F., Savage, N.S., and Lew, D.J. (2013). Interaction between bud-site selection and polarity-establishment machineries in budding yeast. Philos. Trans. R. Soc. Lond. B Biol. Sci. 368, 20130006.

15. Watson, L.J., Rossi, G., and Brennwald, P. (2014). Quantitative analysis of membrane trafficking in regulation of Cdc42 polarity. Traffic 15, 1330–1343.

16. Wu, C.F., Chiou, J.G., Minakova, M., Woods, B., Tsygankov, D., Zyla, T.R., Savage, N.S., Elston, T.C., and Lew, D.J. (2015). Role of competition between polarity sites in establishing a unique front. eLife 4, e11611.

17. Howell, A.S., Jin, M., Wu, C.F., Zyla, T.R., Elston, T.C., and Lew, D.J. (2012). Negative feedback enhances robustness in the yeast polarity establishment circuit. Cell 149, 322–333.

18. Kuo, C.C., Savage, N.S., Chen, H., Wu, C.F., Zyla, T.R., and Lew, D.J. (2014). Inhibitory GEF phosphorylation provides negative feedback in the yeast polarity circuit. Curr. Biol. 24, 753–759.

19. Pruyne, D., Gao, L., Bi, E., and Bretscher, A. (2004). Stable and dynamic axes of polarity use distinct formin isoforms in budding yeast. Mol. Biol. Cell 15, 4971–4989.

20. Chen, H., Kuo, C.C., Kang, H., Howell, A.S., Zyla, T.R., Jin, M., and Lew, D.J. (2012). Cdc42p regulation of the yeast formin Bni1p mediated by the effector Gic2p. Mol. Biol. Cell 23, 3814–3826.

21. Donovan, K.W., and Bretscher, A. (2012). Myosin-V is activated by binding secretory cargo and released in coordination with Rab/exocyst function. Dev. Cell 23, 769–781.

22. Vallen, E.A., Caviston, J., and Bi, E. (2000). Roles of Hof1p, Bni1p, Bnr1p, and myo1p in cytokinesis in Saccharomyces cerevisiae. Mol. Biol. Cell 11, 593–611.

23. Kadota, J., Yamamoto, T., Yoshiuchi, S., Bi, E., and Tanaka, K. (2004). Septin ring assembly requires concerted action of polarisome components, a PAK kinase Cla4p, and the actin cytoskeleton in Saccharomyces cerevisiae. Mol. Biol. Cell 15, 5329–5345.

24. Harrison, J.C., Bardes, E.S., Ohya, Y., and Lew, D.J. (2001). A role for the Pkc1p/Mpk1p kinase cascade in the morphogenesis checkpoint. Nat. Cell Biol. 3, 417–420.

25. Bellí, G., Garí, E., Aldea, M., and Herrero, E. (2001). Osmotic stress causes a G1 cell cycle delay and downregulation of Cln3/Cdc28 activity in Saccharomyces cerevisiae. Mol. Microbiol. 39, 1022–1035.

26. Siede, W., Friedberg, A.S., Dianova, I., and Friedberg, E.C. (1994). Characterization of G1 checkpoint control in the yeast Saccharomyces cerevisiae following exposure to DNA-damaging agents. Genetics 138, 271–281.

27. Nunes, E., and Siede, W. (1996). Hyperthermia and paraquat-induced G1 arrest in the yeast Saccharomyces cerevisiae is independent of the RAD9 gene. Radiat. Environ. Biophys. 35, 55–57.

28. Costanzo, M., Nishikawa, J.L., Tang, X., Millman, J.S., Schub, O., Breitkreuz, K., Dewar, D., Rupes, I., Andrews, B., and Tyers, M. (2004). CDK activity antagonizes Whi5, an inhibitor of G1/S transcription in yeast. Cell 117, 899–913.

29. de Bruin, R.A., McDonald, W.H., Kalashnikova, T.I., Yates, J., 3rd, and Wittenberg, C. (2004). Cln3 activates G1-specific transcription via phosphorylation of the SBF bound repressor Whi5. Cell 117, 887–898.

30. Tiedje, C., Sakwa, I., Just, U., and Höfken, T. (2008). The Rho GDI Rdi1 regulates Rho GTPases by distinct mechanisms. Mol. Biol. Cell 19, 2885–2896.

31. Das, A., Slaughter, B.D., Unruh, J.R., Bradford, W.D., Alexander, R., Rubinstein, B., and Li, R. (2012). Flippase-mediated phospholipid asymmetry promotes fast Cdc42 recycling in dynamic maintenance of cell polarity. Nat. Cell Biol. 14, 304–310.

32. Haruki, H., Nishikawa, J., and Laemmli, U.K. (2008). The anchor-away technique: rapid, conditional establishment of yeast mutant phenotypes. Mol. Cell 31, 925–932.

33. Kozubowski, L., Saito, K., Johnson, J.M., Howell, A.S., Zyla, T.R., and Lew, D.J. (2008). Symmetry-breaking polarization driven by a Cdc42p GEF-PAK complex. Curr. Biol. 18, 1719–1726.

34. Goryachev, A.B., and Pokhilko, A.V. (2008). Dynamics of Cdc42 network embodies a Turing-type mechanism of yeast cell polarity. FEBS Lett. 582, 1437–1443.

35. Savage, N.S., Layton, A.T., and Lew, D.J. (2012). Mechanistic mathematical model of polarity in yeast. Mol. Biol. Cell 23, 1998–2013.

36. Marquitz, A.R., Harrison, J.C., Bose, I., Zyla, T.R., McMillan, J.N., and Lew, D.J. (2002). The Rho-GAP Bem2p plays a GAP-independent role in the morphogenesis checkpoint. EMBO J. 21, 4012–4025.

37. Bender, A., and Pringle, J.R. (1991). Use of a screen for synthetic lethal and multicopy suppressee mutants to identify two new genes involved in morphogenesis in Saccharomyces cerevisiae. Mol. Cell. Biol. 11, 1295–1305.

38. Gong, T., Liao, Y., He, F., Yang, Y., Yang, D.D., Chen, X.D., and Gao, X.D. (2013). Control of polarized growth by the Rho family GTPase Rho4 in budding yeast: requirement of the N-terminal extension of Rho4 and regulation by the Rho GTPase-activating protein Bem2. Eukaryot. Cell 12, 368–377.

39. Lin, Q., Fuji, R.N., Yang, W., and Cerione, R.A. (2003). RhoGDI is required for Cdc42-mediated cellular transformation. Curr. Biol. 13, 1469–1479.

40. Smith, G.R., Givan, S.A., Cullen, P., and Sprague, G.F., Jr. (2002). GTPase-activating proteins for Cdc42. Eukaryot. Cell 1, 469–480.

41. Schmidt, A., Schmelzle, T., and Hall, M.N. (2002). The RHO1-GAPs SAC7, BEM2 and BAG7 control distinct RHO1 functions in Saccharomyces cerevisiae. Mol. Microbiol. 45, 1433–1441.

42. Lorberg, A., Schmitz, H.P., Jacoby, J.J., and Heinisch, J.J. (2001). Lrg1p functions as a putative GTPase-activating protein in the Pkc1p-mediated cell integrity pathway in Saccharomyces cerevisiae. Mol. Genet. Genomics 266, 514–526.

43. Dyer, J.M., Savage, N.S., Jin, M., Zyla, T.R., Elston, T.C., and Lew, D.J. (2013). Tracking shallow chemical gradients by actin-driven wandering of the polarization site. Curr. Biol. 23, 32–41.

44. Irazoqui, J.E., Gladfelter, A.S., and Lew, D.J. (2003). Scaffold-mediated symmetry breaking by Cdc42p. Nat. Cell Biol. 5, 1062–1070.

45. Layton, A.T., Savage, N.S., Howell, A.S., Carroll, S.Y., Drubin, D.G., and Lew, D.J. (2011). Modeling vesicle traffic reveals unexpected consequences for Cdc42p-mediated polarity establishment. Curr. Biol. 21, 184–194.

46. Wu, C.F., and Lew, D.J. (2013). Beyond symmetry-breaking: competition and negative feedback in GTPase regulation. Trends Cell Biol. 23, 476–483.

47. Delley, P.A., and Hall, M.N. (1999). Cell wall stress depolarizes cell growth via hyperactivation of RHO1. J. Cell Biol. 147, 163–174.

48. Silvius, J.R., and l'Heureux, F. (1994). Fluorimetric evaluation of the affinities of isoprenylated peptides for lipid bilayers. Biochemistry 33, 3014–3022.

49. Ghomashchi, F., Zhang, X., Liu, L., and Gelb, M.H. (1995). Binding of prenylated and polybasic peptides to membranes: affinities and intervesicle exchange. Biochemistry 34, 11910–11918.

50. Moissoglu, K., Slepchenko, B.M., Meller, N., Horwitz, A.F., and Schwartz, M.A. (2006). In vivo dynamics of Rac-membrane interactions. Mol. Biol. Cell 17, 2770–2779.

51. Boulter, E., Garcia-Mata, R., Guilluy, C., Dubash, A., Rossi, G., Brennwald, P.J., and Burridge, K. (2010). Regulation of Rho GTPase crosstalk, degradation and activity by RhoGDI1. Nat. Cell Biol. 12, 477–483.